

Calibration of Fish-Eye Stereo Camera for Aurora Observation

Yoshiki Mori¹, Atsushi Yamashita², Masayuki Tanaka³, Ryuho Kataoka³
Yoshizumi Miyoshi⁴, Toru Kaneko¹, Masatoshi Okutomi³, Hajime Asama²

¹ Graduate School of Engineering, Shizuoka University, 3-5-1 Johoku, Naka-ku, Hamamatsu-shi, Shizuoka, Japan

² School of Engineering, The University of Tokyo, 7-3-1 Hongo, Bunkyo-ku, Tokyo, Japan

³ Graduate School of Engineering, Tokyo Institute of Technology, 2-12-1 Ookayama, Meguro-ku, Tokyo, Japan

⁴ Solar-Terrestrial Environment Laboratory, Nagoya University, Furo-cho, Chikusa-ku, Nagoya, Japan

Email: f0230068@ipc.shizuoka.ac.jp

Abstract—Three-dimensional measurement of aurora, including its altitude is so difficult that it has not been done before. In this paper, we propose to observe aurora using a fish-eye stereo camera system which can acquire a panoramic view of the sky in a single shot. Stereo observation needs the information of posture of each camera constructing a stereo system. Therefore, we propose a method to estimate the posture of the camera by using stars as calibration targets. Experiments show the effectiveness of the proposed method.

Keywords: Aurora, Stereo, Fish-eye camera, Calibration.

I. INTRODUCTION

Aurora occurs at an altitude of about 100~200km above the ground by the interaction between the precipitating particles and the upper atmosphere. Its shape reflects the mechanism that produces aurora. Therefore, three-dimensional measurement of aurora is important for estimation of auroral electron energy spectrum. However, continuous observation of a three-dimensional shape of aurora is so difficult that it has not been done before. Therefore, we propose a method for three-dimensional measurement of aurora including the altitude above the ground using a stereo camera system.

A fish-eye camera with a wide field of view makes it possible to measure a wide range. In this study, we propose a method to observe aurora using a fish-eye stereo camera system which can acquire the panoramic view of the sky in a single shot. Fig. 1 shows aurora images obtained at Poker Flat Research Range, University of Alaska, Fairbanks, by Aurora 3D project (aurora3d.jp). In the project, two cameras are set in the distance of about 3km, and observe aurora occurring over 100km (Fig. 2).

Stereo observation needs internal and external parameters of each camera which constructs a stereo system. The internal parameters include the center of the image and the focal length. The external parameters are concerning to position and posture of the camera. The internal parameters are obtained by calibration using specific observation patterns.

The position of the camera is determined by attaching a GPS receiver to the camera. Therefore, in this paper we propose a method to estimate the posture of the camera.

Studies on projection models and calibration of the fish-eye camera have been made [1][2][3]. In addition, a calibration

method using the image of the night sky is proposed [4]. Then, we propose a method to estimate the posture of the camera by using stars as calibration targets.

II. FISH-EYE LENS MODEL

A fish-eye camera has a hemispherical field of view. Generally, the fish-eye camera is composed of a fish-eye lens mounted on a normal camera. Fish-eye lens models are classified according to projection methods, such as equidistant projection whose resolution does not depend on the angle of view and equisolid angle projection in which the ratio of an incident solid angle and its resulting area in an image is constant. The fish-eye lens model used in this study is equisolid angle projection, which is represented by the following equation (Fig. 3)

$$r = 2f \sin \frac{\theta}{2} \quad (1)$$

where r is the distance from a pixel to the image center (C_u, C_v) , θ is the angle from the optical axis of the camera, and f is the focal length.

III. METHOD OF CAMERA PARAMETER ESTIMATION

Camera parameters are classified into internal parameters and external parameters. The parameters to estimate in this paper are image center (C_u, C_v) and the focal length f for the internal parameters, and camera posture around the X-, Y-, and Z-axes for the external parameters, as shown in Table I



(a) Camera A

(b) Camera B

Fig. 1. Captured image

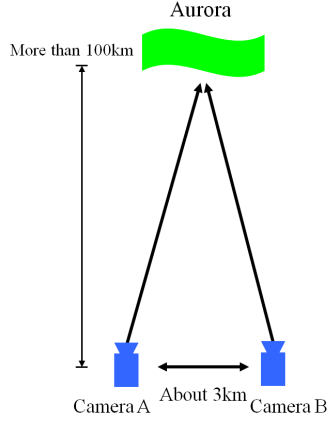


Fig. 2. Observation geometry

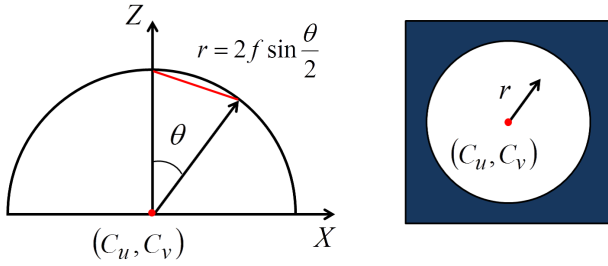


Fig. 3. Equisolid angle projection

A. Internal camera parameters

An image of a check pattern as shown in Fig. 4 is taken by the camera to estimate the image center by using the OcamCalib Toolbox [5]. The focal length is estimated by using a linear pattern image [6] as shown in Fig. 5. We estimate the image coordinates of 90 degrees from the optical axis of the camera. Then, the focal length f is determined by substituting the distance from the center of the image to the estimated image coordinates and $\theta = 90 \text{ deg}$ for (1).

B. External camera parameters

External parameters of the camera are its position and posture. In this study, the position of the camera is obtained by attaching a GPS receiver to the camera. Therefore, we should only estimate the posture of the camera.

1) *Rectified coordinate system*: In this study, we define a coordinate system as follows. The origin of the coordinate system is the optical center of each camera. The X-axis is directed from the optical center of Camera A to that of Camera B. The Y-axis, lying in the horizontal plane, is directed perpendicular

TABLE I
CAMERA PARAMETERS TO ESTIMATE

Parameter	Content
Internal parameters	Image center (C_u, C_v)
	focal length f
External parameters	Posture around X-, Y-, and Z-axes

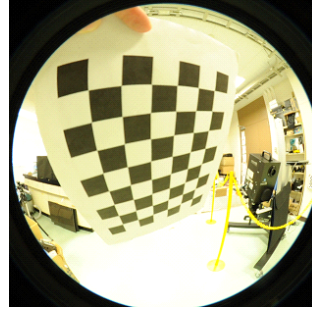


Fig. 4. Calibration pattern for estimation of the image center.

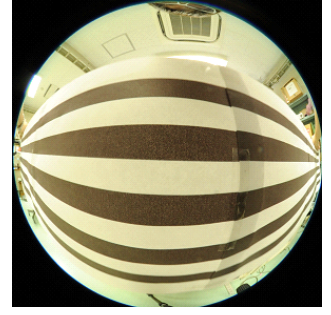


Fig. 5. Calibration pattern for estimation of the focal length.

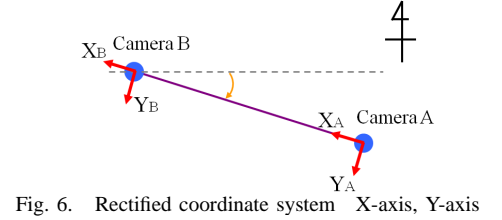


Fig. 6. Rectified coordinate system (X-axis, Y-axis)

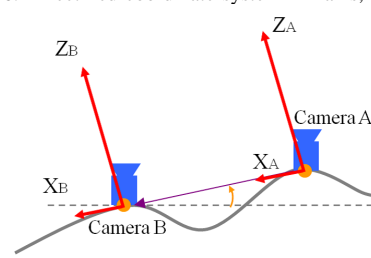


Fig. 7. Rectified coordinate system (X-axis, Z-axis)

to the X-axis and forms a right handed system. The Z-axis is directed outward from the Earth and perpendicular to both X-axis and Y-axis. We define this coordinate system as the rectified coordinate system. Fig. 6 and 7 show the directions of the axes of the rectified coordinate system. The direction of a star in the rectified coordinate system is calculated from its right ascension and declination, the position of the camera, and the observation date and time.

2) *Direction vector calculation from images of stars*: In the proposed method, the camera posture is estimated by using the direction vector of stars. The direction vector $(x, y, z)^T$ is determined if θ and ϕ in Fig. 8 are obtained. If we denote the image coordinates and the distance from the image center by (u, v) and r , respectively, we have the following equation.

$$r = \sqrt{(u - C_u)^2 + (v - C_v)^2} \quad (2)$$

Then, the angle θ from the optical axis is calculated from (1). Further, the angle ϕ from the X-axis is calculated from the following equations.

$$\sin \phi = \frac{u - C_u}{r} \quad (3)$$

$$\cos \phi = \frac{v - C_v}{r} \quad (4)$$

The direction vector $(x, y, z)^T$ is obtained from the following equation.

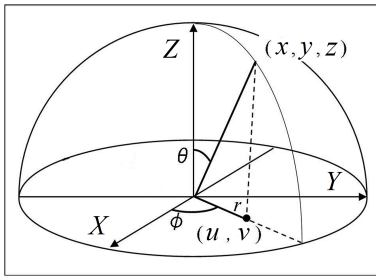


Fig. 8. Direction vector of a star

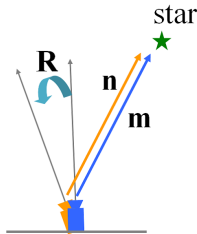


Fig. 9. Camera posture and direction vector of a star.

$$\begin{bmatrix} x \\ y \\ z \end{bmatrix} = \begin{bmatrix} \sin \theta \cos \phi \\ \sin \theta \sin \phi \\ \cos \theta \end{bmatrix} \quad (5)$$

3) *Method of camera posture estimation:* The camera posture is represented both in the rectified coordinate system and in the actual coordinate system of the camera as shown in Fig. 9, where the former and the latter coordinate systems are drawn in blue and yellow, respectively. The true value of the direction vector of a star in the rectified coordinate system can be calculated from the observation date/time and position. The direction vector of a star in the camera coordinate system is calculated from the image coordinates of the captured image. If we represent the direction vectors of a star in the rectified coordinate system and in the actual coordinate system of the camera by \mathbf{m} and \mathbf{n} respectively (blue line and yellow line in Fig. 9), each camera has the following equation.

$$\mathbf{n} = \mathbf{R}\mathbf{m} \quad (6)$$

where \mathbf{R} is a rotation matrix between the two coordinate systems.

Equation (6) holds for each camera, and then rotation matrices \mathbf{R}_A and \mathbf{R}_B between the two coordinate systems for each camera can be estimated independently. Then, we find the optimum rotation matrix by minimizing (7) with vector pairs of N number of stars for each camera.

$$E = 1 - \frac{1}{N} \sum_{k=1}^N (\mathbf{n}_k^T \mathbf{R} \mathbf{m}_k) \quad (7)$$

where \mathbf{m}_k and \mathbf{n}_k are k -th vector pairs of \mathbf{m} and \mathbf{n} , respectively.

IV. EXPERIMENTS

A. System overview

Aurora observation was carried out with two sets of observation devices set up in Alaska. The set was composed of an uninterruptible power supply (UPS), PC, a fish-eye camera and a hard disk for data storage, and put in the case for outdoor observation as shown in Fig. 10 which is accommodated in all sky dome of observatory. The positions of the camera with a GPS receiver were recorded in the WGS-84 coordinate. The obtained data are shown in Table II. The distance between the two fish-eye cameras is about 3km. The angle between the latitude line and the X-axis (Fig. 6) was 16.014 degrees, and the angle between the horizontal plane and the X-axis (Fig. 7) was 5.670 degrees.

TABLE II
LATITUDE, LONGITUDE AND ALTITUDE OF THE CAMERA

	Camera A	Camera B
Latitude	N 65 °07 7.128	N 65 °07 35.766
Longitude	W 147 °25 58.008	W 147 °29 47.982
Altitude	516m	205m

B. Camera parameter estimation

1) *Simulation:* Before estimating the rotation matrix from the actually captured images, a simulation was performed in order to verify the validity of the proposed method. The simulation used the image shown in Fig. 11. The image size was 180×180 pixels. The number of stars used to estimate was 20. The coordinates of the image center was set to (90, 90) and the focal length was set to 63.634.



Fig. 10. Observation devices

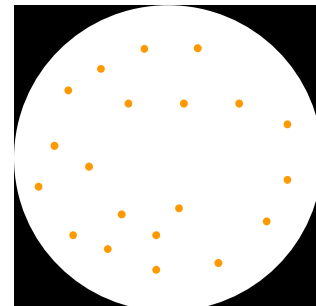
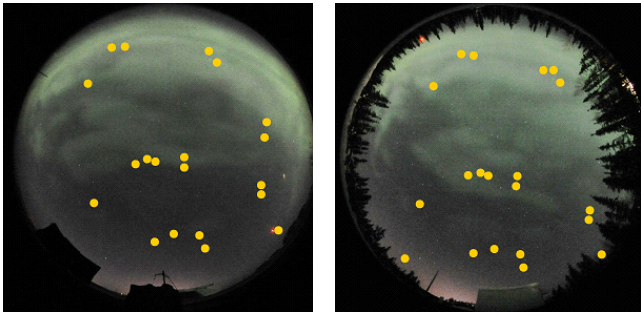


Fig. 11. Simulation image



(a) Camera A (b) Camera B

Fig. 12. The coordinates of the star

The true value of Rotation matrix \mathbf{R}_t was as follows.

$$\mathbf{R}_t = \begin{bmatrix} 0.935755 & -0.302933 & -0.180540 \\ 0.283165 & 0.950581 & -0.127335 \\ 0.210192 & 0.068031 & 0.975290 \end{bmatrix} \quad (8)$$

In comparison, the rotation matrix obtained as a result of estimation was as follows.

$$\mathbf{R} = \begin{bmatrix} 0.935755 & -0.302933 & -0.180540 \\ 0.283165 & 0.950581 & -0.127335 \\ 0.210192 & 0.068031 & 0.975290 \end{bmatrix} \quad (9)$$

Because the estimation result was consistent with the true value, we confirmed that the proposed method can estimate the rotation matrix representing the camera posture.

2) *Results using actual images*: Images taken in Alaska were used to estimate the rotation matrix. The image size was 2784×1848 pixels. The number of stars used to estimate was 20. Fig. 12 is a chart obtained by plotting the coordinates of the stars used to estimate as yellow points.

Table III shows the image coordinates and the names of the stars used to estimate.

We had no on-site information of the internal parameters of the camera used in Alaska. Therefore, tentative internal parameters were determined for a camera configuration in which the same lens used in the actual aurora observation was mounted on another camera body. The coordinates of the image center was (1360.70, 933.75) and the focal length was 519.02.

Experimental results were as follows.

$$\mathbf{R}_A = \begin{bmatrix} 0.983326 & 0.145196 & 0.109489 \\ -0.165367 & 0.964433 & 0.206212 \\ -0.075653 & -0.220880 & 0.972362 \end{bmatrix} \quad (10)$$

$$\mathbf{R}_B = \begin{bmatrix} 0.946128 & 0.286162 & 0.151501 \\ -0.297000 & 0.953347 & 0.054044 \\ -0.128967 & -0.096128 & 0.986979 \end{bmatrix} \quad (11)$$

Table IV shows the average angular error of the direction vectors of the stars, the average pixel error in the image, and the error in the depth direction when measuring an object at 100km above the ground with the average angle error.

An experimental result is shown in Fig. 13 where green points and red points are drawn on a night sky image to indicate the angular positions of direction vectors given by

TABLE III
THE IMAGE COORDINATES AND THE NAME OF THE STAR

The name of the star	Camera A	Camera B
	Coordinates(u, v)	Coordinates(u, v)
Vega	(1027,581)	(1093,593)
Deneb	(1203,405)	(1284,447)
Sadr	(1140,409)	(1225,440)
Arcturus	(1056,1149)	(1028,1154)
Denebola	(1344,1334)	(1283,1388)
Spica		(957,1413)
Zosma	(1434,1296)	(1382,1368)
Algieba	(1556,1303)	(1506,1393)
Regulus	(1583,1365)	(1521,1456)
Alkaid	(1253,964)	(1258,1017)
Mizar	(1308,940)	(1317,1005)
Alioth	(1347,952)	(1354,1019)
Merak	(1484,980)	(1486,1069)
Dubhe	(1484,931)	(1492,1021)
Schedar	(1601,426)	(1664,517)
Ruchbah	(1639,480)	(1696,576)
Capella	(1875,764)	
Menkalinan	(1865,837)	
Castor	(1849,1064)	(1837,1184)
Pollux	(1849,1108)	(1832,1229)
Procyon	(1931,1279)	(1893,1394)
Caph		(1616,517)

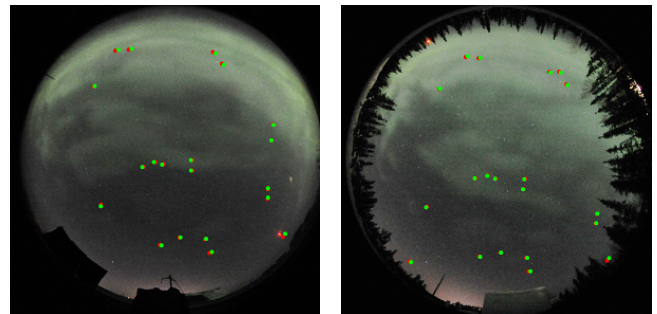
TABLE IV
ANGULAR ERROR

	Camera A	Camera B
The average angular error	0.84deg	0.57deg
Pixel error in the image	About 15pixel	About 10pixel
Error in the depth direction	About 33km	About 25km

\mathbf{n} and \mathbf{Rm} respectively. The closer the green points and red points are to one another, the more accurately the estimation of \mathbf{R} is evaluated.

Deviation between red points and green points could not be reduced by a simple operation such as translation or rotation. There was also a tendency that the amount of deviation grows increasingly according to the distance from the center of the image.

A cause of the error might be the use of the tentative internal parameters of the camera instead of the true parameters. Another cause might be the effect of light refraction. Stars near the horizon are subject to atmospheric refraction (Fig. 14). In



(a) Camera A (b) Camera B

Fig. 13. Experimental result

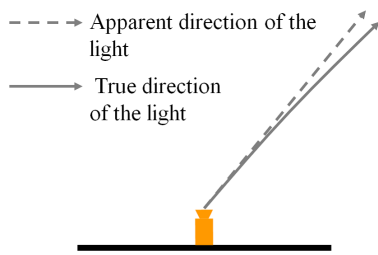


Fig. 14. Atmospheric refraction

addition, the observation set has a hemispherical transparent dome-shaped cover over the camera, and the optical axis of the camera and the center of the cover cannot be expected to coincide with each other. Therefore, there is a possibility that deviation occurs by refraction of light rays through the cover.

C. Image conversion

Using the results of the experiments, we converted the observed stereo images. Image conversion was performed so as to convert the captured images into those represented in the rectified coordinate system. Fig. 15 shows images before conversion and Fig. 16 shows the results of image conversion. We projected these images in Synra Dome which is a facility to project three-dimensional images in Science Museum. By comparison of the images before and after the conversion, we confirmed that the converted images are more effective for our stereoscopic perception.

V. CONCLUSION

A method to estimate postures of a fish-eye stereo camera system for aurora observation is proposed. The method uses stars as calibration targets. We confirmed the effectiveness of the proposed method by experiment.

As future work to improve the observation accuracy, we should estimate internal parameters with images taken in a real environment. We should also consider the refraction of light rays by atmosphere and the cover of the camera.

ACKNOWLEDGMENT

In conduct of study, we deeply appreciate the permission to use Poker Flat Research Range, University of Alaska Fairbanks, and the cooperation of Prof. Don Hampton and staffs.

We also deeply appreciate Nikon Imaging Japan Inc. for providing us camera equipment, Mr. Toshiyuki Takahei, ORIHALCON Project, and Mr. Wataru Fujishige, Science Museum, for their cooperation.

A part of this study was funded by the Asahi Glass Foundation and the Hosono Bunka Foundation in FY2010 and FY2011.

REFERENCES

- [1] K. Miyamoto: "Fish Eye Lens," *Journal of the Optical Society of America*, Vol. 54, No. 8, pp. 1060–1061, 1964.
- [2] S. Shah and J. K. Aggarwal: "Intrinsic Parameter Calibration Procedure for a (High-Distortion) Fish-Eye Lens Camera with Distortion Model and Accuracy Estimation," *Pattern Recognition*, Vol. 29, pp. 1775–1788, 1996.
- [3] C. Hughes, P. Denny, E. Jones and M. Glavin: "Accuracy of Fish-eye Lens Models," *Applied Optics*, Vol. 49, No. 17, pp. 3338–3347, 2010.
- [4] A. Klaus, J. Bauer, K. Karner, P. Elbischger, R. Perko and H. Bischof: "Camera Calibration from a Single Night Sky Image," *Proceeding of the 2004 IEEE Computer Society Conference on Computer Vision and Pattern Recognition (CVPR2004)*, Vol. 1, pp. 151–157, 2004.
- [5] D. Scaramuzza, A. Martinelli and R. Siegwart: "A Toolbox for Easy Calibrating Omnidirectional Cameras," *Proceeding of the 2006 IEEE/RSJ International Conference on Intelligent Robots and Systems (IROS2006)*, pp. 5695–5701, 2006.
- [6] M. Nakano, S. Li and N. Chiba: "Calibrating Fisheye Camera By Stripe Pattern Based upon Spherical Model," *The Transactions of the Institute of Electronics, Information and Communication Engineers D*, Vol. J90-D, No. 1, pp. 73–82, 2007 (in Japanese).

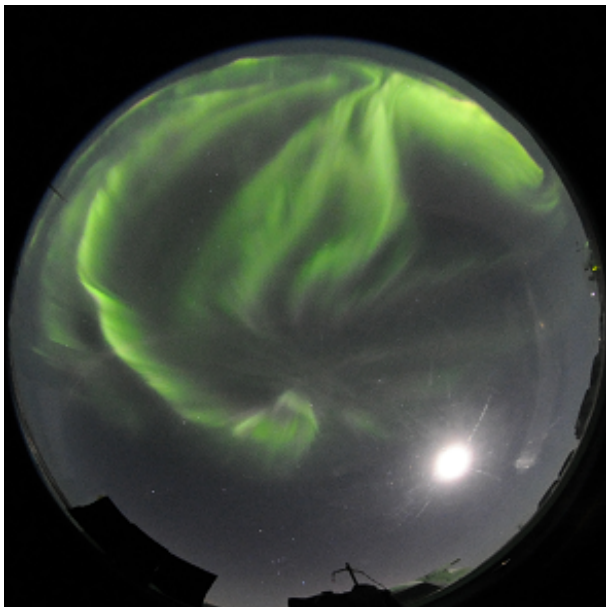


(a) Camera A



(b) Camera B

Fig. 15. Image before conversion



(a) Camera A



(b) Camera B

Fig. 16. Results of image conversion